This is a repository copy of *Experimental validation of Viper underwater explosion CFD solver*.

White Rose Research Online URL for this paper:
https://eprints.whiterose.ac.uk/220929/

Version: Accepted Version

Proceedings Paper:
Farrimond, D. orcid.org/0000-0002-9440-4369, Nicholson, A., Nowak, P. et al. (9 more authors) (2024) Experimental validation of Viper underwater explosion CFD solver. In: Proceedings of The 19th International Symposium on Interaction of the Effects of Munitions with Structures (ISIEMS). 19th International Symposium on Interaction of the Effects of Munitions with Structures (ISIEMS), 09-13 Dec 2024, Bonn, Germany. International Symposium on Interaction of the Effects of Munitions with Structures (ISIEMS)

© 2024 ISIEMS. This is an author-produced version of a paper subsequently published in Proceedings of The 19th International Symposium on Interaction of the Effects of Munitions with Structures (ISIEMS). Uploaded with permission from the copyright holder.

Reuse
Items deposited in White Rose Research Online are protected by copyright, with all rights reserved unless indicated otherwise. They may be downloaded and/or printed for private study, or other acts as permitted by national copyright laws. The publisher or other rights holders may allow further reproduction and re-use of the full text version. This is indicated by the licence information on the White Rose Research Online record for the item.

Takedown
If you consider content in White Rose Research Online to be in breach of UK law, please notify us by emailing eprints@whiterose.ac.uk including the URL of the record and the reason for the withdrawal request.

eprints@whiterose.ac.uk
https://eprints.whiterose.ac.uk/

Distribution: For public release

Experimental Validation of Viper Underwater Explosion CFD Solver

Dain Farrimond[1,4], Andrew Nicholson[2], Piotr Nowak[3], Lewis Tetlow[1,4], Adam Dennis[1], Tommy Lodge[1,4], Genevieve Langdon[1], Andy Tyas[1,4], Piotr Sielicki[3], Tomasz Gajewski[3], Peter McDonald[2], Chris Stirling[2]

1 University of Sheffield, United Kingdom

2 Viper Applied Science, United Kingdom

3 Poznan University of Technology, Poland

4 Blastech Ltd, United Kingdom

Keywords: Blast, underwater, Characterisation, Variability, CFD, Simulation, Modelling, UNDEX

Abstract

In the last few decades, the situation on the water edges of the NATO borders proved that there is a growing need for accurate modelling of underwater explosive events. Traditionally, predicting loading conditions for these events relied on CPU-based solving tools, which, while effective, often required significant computational resources and time. Viper::Blast has now been extended to include a novel underwater explosive CFD prediction tool, leveraging advanced GPU technologies to enhance performance and reduce computation times.

This paper evaluates the capability of the Viper::Blast underwater explosive CFD prediction tool by comparing its results with well-controlled experimental data. The comparison focuses on key metrics such as pressure, impulse, and wave propagation in underwater environments. By assessing the accuracy and efficiency of Viper::Blast in these scenarios, the paper demonstrates its potential as a reliable and fast alternative to traditional CPU-based methods for underwater blast modelling.

Introduction

Computational Fluid Dynamic (CFD) solvers offer great potential for modelling blast phenomena, providing detailed insights into the complex interactions during such events. Recently, the run times of these solvers have been dramatically reduced through the integration of modern GPU technologies, enabling more efficient and rapid computations. Viper Applied Science has developed a fast-running air-blast CFD solving tool, Viper::Blast, which has been well validated against results from air-blast experiments [1,2].

Explosions in media other than air are inherently more complex modelling types. For example, when the explosive is surrounded by multiple (solid) materials, the variations in material stiffness (often characterised by Elastic modulus or bulk modulus) lead to different wave speeds and characteristic lengths to be implemented within the same model. This in turn implies smaller time increments for software using explicit time integration schemes and hence longer run times and higher computational power requirements. For the underwater regime, this is compounded by the presence of multiple phases as well as multiple materials, e.g. water, solid explosive, gaseous explosive detonation productions, cavitation bubbles and so on.

These complex challenges often lead modellers to consider simpler approaches, such as similitude relations and idealised cases. However, realistic scenarios are seldom similar to the idealised cases, making comparisons difficult and extrapolation questionable. The need for an accurate, versatile CFD solver that operates efficiently to predict underwater blast loads is necessitated by the presence of a water surface for near surface drones, weapons and unexploded ordnance as similitude rules and adjustments break down in these regimes. None of these is well captured by idealised cases but the extent to which the simplistic models are reliable cannot be assessed without alternative reliable predictions for complex scenarios. However, understanding these loading types is essential as they represent realistic threats to infrastructure and assessments of their potential risk is vital for improved infrastructure resilience, hazard modelling and human injury risk reduction.

Nowak et al [3] conducted a review of historical large scale underwater experimental trials and conducted similar experiments in which reasonable repeatability or comparability to CFD simulation or empirical fits at larger standoff distances was not achieved. Continuation of this work looked to reduce the scales of the trials to increase the level of control over the experimental methodology [4], which when considering bubble dynamics, compared better to simplified empirical predictions provided by Cole et al [5].

This paper evaluates the capability of Viper::Blast's GPU accelerated underwater explosive CFD prediction tool by comparing its results with experimental data taken from tests conducted at The University of Sheffield. The comparison focuses on key metrics such as pressure, impulse, and arrival time to critically evaluate the model’s ability to capture wave propagation in underwater environments. By assessing the accuracy and efficiency of Viper::Blast in these scenarios, the paper demonstrates its potential as a reliable and fast alternative to traditional CPU-based methods for underwater blast modelling.

University of Sheffield Experimental Setup and Instrumentation

Figure 1 presents a schematic of the UNDEX facility based at the University of Sheffield, which consists of a 2m diameter, 2m tall cylindrical open topped tank. The tank can be filled with water and varying strata. Portholes are fitted to the sides of the tank to allow for optical High-Speed Video (HSV) recordings. Sufficient clarity of water (to capture HSV footage) is achieved using an overflowing action of a receptacle during pumping.

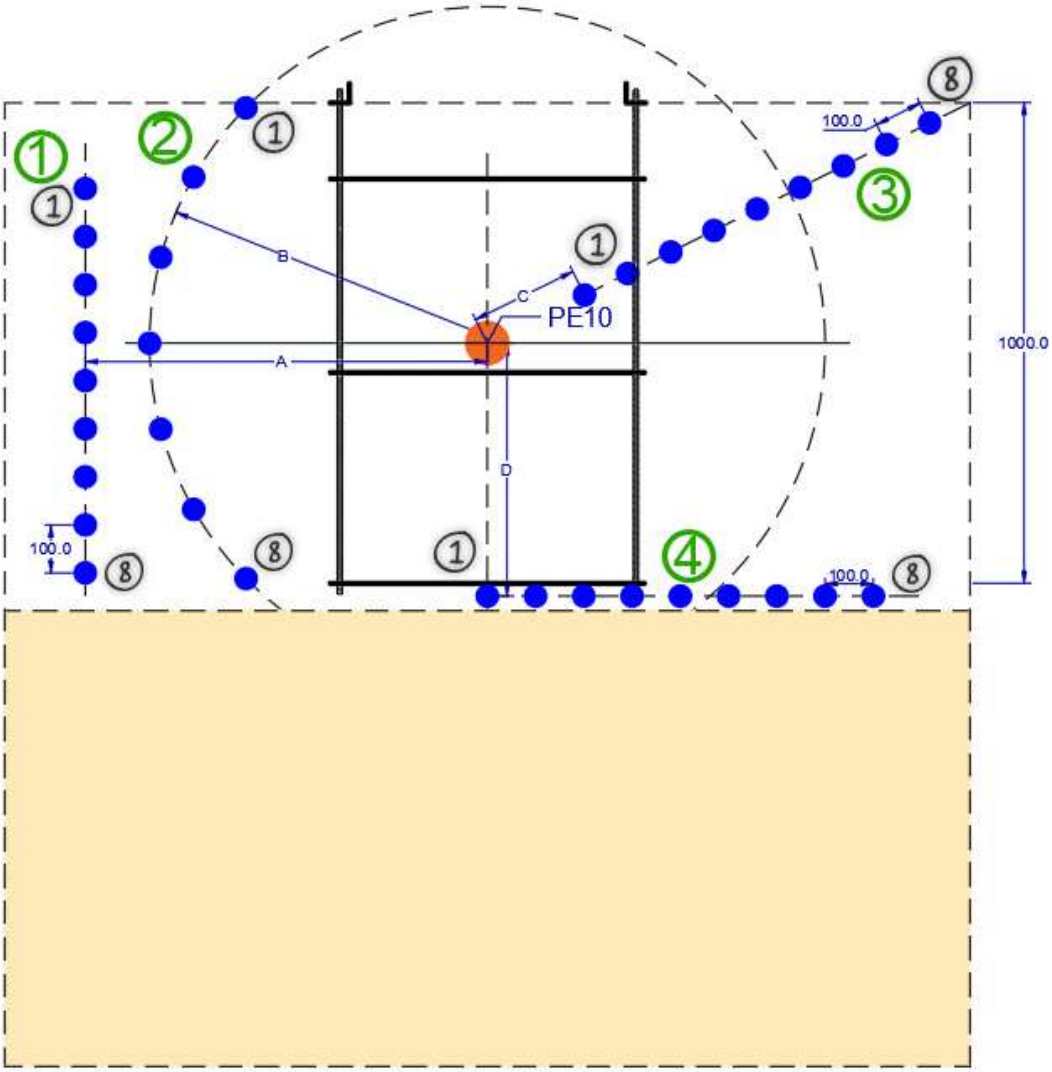

Figure 1. Schematic showing the structural gauge mounting method adopted for the tests used for validation within this paper with green numbering denoting the gauge position layouts.

The facility has been used for 39 trials with varied gauge positions and charge sizes to provide a total of 341 individual pressure-time history recordings. These trials are discussed in Farrimond et al. [6] where additional information regarding the experimental data analysis and repeatability of underwater blast loading is discussed.

Throughout this study, six independent trials have been identified as validation data for the newly developed Viper::Blast underwater explosion solver. These tests included detonating

spheres of PE10 explosive (86% PETN, 14% binder-plasticizer, TNTe=1.22 [7]) with masses ranging from 5 to 20g. In all instances the charge was placed at the centre of the tank on plan, and at half depth in the water. Each charge was centrally detonated using a Euronel non-electrical detonator (0.8 g TNT equivalent mass of explosive).

Within the overall study [6], a combination of PCB 138A10 underwater blast transducers and Neptune T11 shock gauge transducers were utilised to compare recorded measurements from two different gauge providers and construction types. They were positioned such that a spatial map of the variation of the blast parameters could be extracted from the tank. A Line-powered ICP sensor signal conditioner Model 482C05 and Kistler LabAmp Type 5165A4 were utilised respectively to power the pressure gauges with no additional pre-filtering applied to any of the signals.

The gauges were placed within the water with scaled distances ranging between 1.0–6.5 $m/kg^{1/3}$ from the explosive itself. Recordings were triggered off a breakwire signal (the breakwire itself was wrapped around the detonator) using a 16-bit digital oscilloscope and TiePie software, with an average sampling rate of 131k samples at a rate of 1MHz.

Simulation Software

The conservation equations considered within the Viper::Blast solver are the Euler equations with the assumption that the gases and liquids are inviscid. Therefore, turbulence or shear waves are not of principal concern. Various explicit numerical integration options are available, including Runga-Kutta integration and traditional second order accurate two step schemes. Spatial discretisation can employ a variety of limiters for 2nd or higher orders of interpolation of cell centred values to the cell edges. Limiters are Total Variation Diminishing (TVD) in nature applying the higher order interpolation only in smooth regions of the flow. The CFD grid for the flow solver is uniform Cartesian. This allows for structured mapping of upstream and downstream cells and efficient memory utilisation.

Meshing of objects or geometry within the solver is performed upon primitive objects such as cuboids, cylinders or wedges. For more detailed objects, STL meshes, or Finite Element meshes can be used with a voxelisation approach to define which cells within the domain contain or do not contain obstacles. By doing so, an effective mapping can be applied to fluxes to embed the geometry within the domain. Boundaries are treated as either transmissive in nature or wholly reflecting. Imposition of the reflecting boundary is complete in the fluxes allow for no flow through the boundary. For transmissive boundaries a ghost cell region is applied to approximate the transmission.

A major advantage of Viper::Blast is that the software is accelerated on Graphical Processing Units (GPUs) for the efficient parallelisation of the computation. Thus, 1000’s of simpler GPU cores can drastically reduce run times when compared to an equivalent method being solved with a Central Processing Unit (CPU).

Numerical Setup

For the purposes of modelling the experimental test series, the domain was separated into multiple phases. This was necessary to simulate the detonation products, the surrounding water and the free surface from the air at the top of the tank independently.

For the detonation products, the typically used JWL equation of state was utilised, derived from equations 1 and 2. Input parameters for the model are also provided and are based upon EXPLO5 derived values for PE10 presented in Table 1 [7].

$$P_{Det\ Products} = A_1\left(1-\frac{w}{R_{1V}}\right)\exp(-R_1V) + A_2\left(1-\frac{w}{R_{2V}}\right)\exp(-R_2V) + \frac{we^*_{Burned}}{V} \quad \textbf{(1)}$$

$$V = \frac{\rho_0}{\rho} \quad \textbf{(2)}$$

Parameter	Value	Unit
Density	1550	Kg/m^3
Energy	5.18e+06	Joules/Kg
A1	3.21e+11	Pa
R1	4.40	Unitless
A2	9.40e+09	Pa
R2	1.228	Unitless
Omega	0.271	Unitless

Table 1. JWL Parameter set for PE10 derived from EXPLO5.

The surrounding water was modelling using the linearised Tillotson equation of state derived from equations 3 and 4. This methodology of simulating water for underwater blasts has been commonly used within published literature [8,9,10] with the parameter set used within this paper being extracted from [8] and presented in Table 2.

$$P_{fluid} = P_0 + (A*\mu) + (B*\mu^2) + (C*\mu^3) + (w*\rho*(e-\ e_0)) \quad \textbf{(3)}$$

$$\mu = \frac{(\rho-\rho_0)}{\rho_0} \quad \textbf{(4)}$$

Parameter	Value	Unit
Density	1000	Kg/m^3
Density 0	1000	Kg/m^3
Omega	0.28	Unitless
A	2.2E+09	Pa
B	9.94e+09	Pa
C	1.457e+10	Pa
Pressure 0	1.00e+05	Pa
Energy	3.542e+05	Joules/Kg
Energy 0	3.542e+05	Joules/Kg

Table 2. Linearised Tillotson equation of state parameters of water [9].

To model the air above the water surface, an ideal gas equation of state was employed using equation 5 along with parameters detailed in Table 3.

$$P_{air} = w * \rho * e \quad \textbf{(5)}$$

Parameter	Value	Unit
Density	1.22	Kg/m^3
Omega	0.4	Unitless
Ambient Pressure	101325.0	Pa

Table 3. Ideal gas equation of state parameters of Air

The model was setup in 2D axisymmetry with a depth dependant pressure gradient and gravity applied. Figure 2 below illustrates the evolution of the pressure wave in the fluid as the pressure expands and reaches the surface causing cavitation and thus a sudden reduction in pressure back to zero as seen in Figure 2a to 2c.

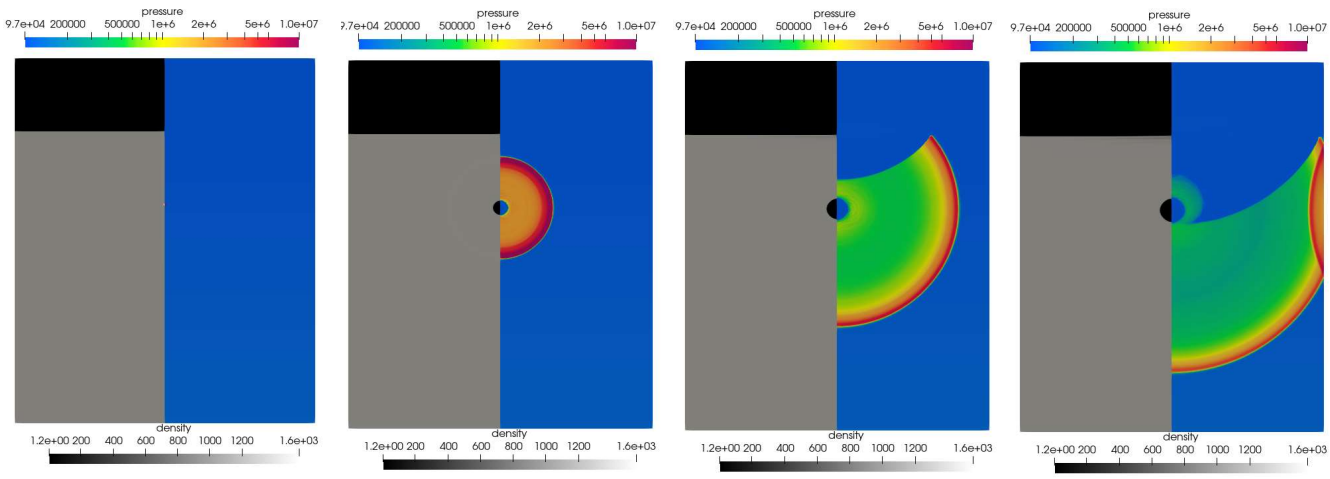

Figure 3. Simulation for 5g PE10 spherical charge detonated 500mm below the surface centrally of the UoS UNDEX tank. Snapshots through time. The left-hand side of Figures illustrates density, whilst the right-hand side shows pressure.

Figure 2d shows the point at which the shock wave arrives at the boundary conditions of the tank extents, where the shock interaction has been simplified and assumed to be perfectly reflected by a rigid wall, therefore omitting energy dissipation during shock interaction.

As mentioned in the experimental methodology, several trials were also conducted with a strata layer being present to a given depth within the tank, thus reducing the height of the water. To remove the need to model saturated strata dynamics, the strata-water interface was assumed to be perfectly rigid. This has been assumed to result in visible longer duration differences in pressure-times histories between the numerical simulation and experimental results. The following sections explore this, and other findings from the comparison.

Numerical to Experimental Comparisons

To validate the simulation behaviour of the Viper::Blast underwater solver, a selection of "simplistic" scenarios were modelled where the tank was filled with 2000mm of water, the explosive was detonated centrally in the tank, and gauges were located at 1000mm depth with three different standoffs (denoted by gauge arrangement 4 in figure 1 but both charge and gauges at 1000mm depth).

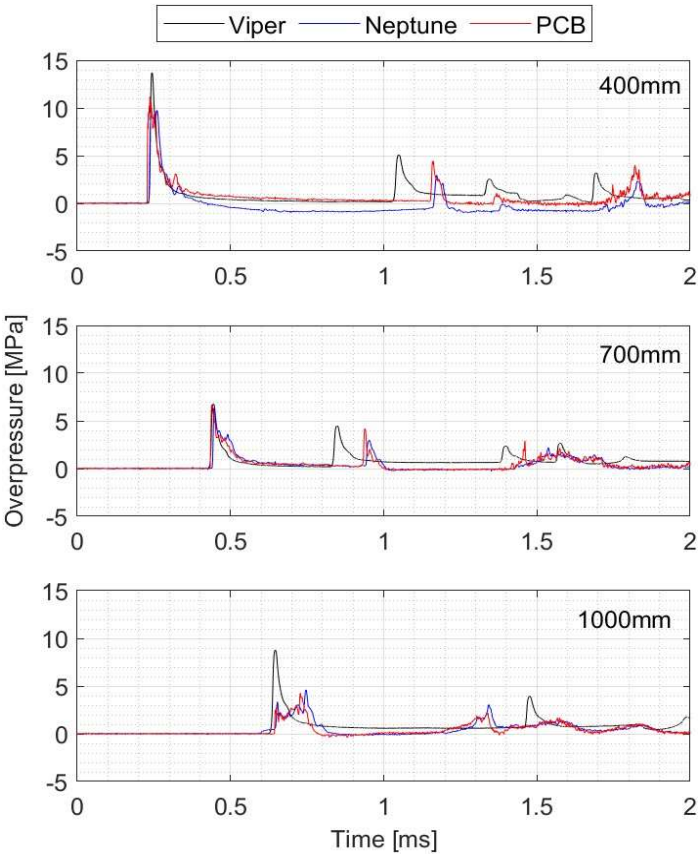

Figure 3. Pressure-time history profiles for 5g PE10 spherical charge detonated centrally of the UoS UNDEX tank filled with 2000mm of water and no strata. Comparisons made between gauge type recordings and Viper UNDEX simulations at three positions of standoff at 1000mm depth.

Qualitatively considering the three standoff positions shown in Figure 3, comparisons can be made between the test pressure gauge type (of two different types) and the Viper::Blast numerical simulation prediction. At 400mm standoff, the arrival of the incident shock and peak overpressure are experimentally and numerically comparable, confidence in the gauge placement (with relation to the charge) and the solvers ability to replicate the detonation process within water. The initial pressure peak and waveform shape are similar, although there are some differences in the arrival time of the secondary pressure pulse, with Viper::Blast predicting a slightly earlier time to secondary peak. Interestingly, the magnitudes of the peaks were comparable. At time = 0.35ms, the Neptune gauge began to drift to a negative pressure which later was investigated to be a result of grounding issues and therefore was omitted from further examination. The PCB gauge and viper traces however have similar trends, but the latter consistently produces larger magnitudes across repeat trials at this standoff which is related to the physical size of the gauge in relation to the arc of the shock wave.

The 1000mm standoff gauge was located as close to the tank wall as feasibly possible and therefore was subjected to reflected shock loading within a short duration after the arrival of the incident shock. The rigidity of the tank within the numerical simulation results in significant differences in the output pressure-time history for the incident shock which is a limitation of these simulations. To improve the accuracy, the structure and fluid interaction behaviour requires a coupled approach, or an approximation of energy dissipation.

This numerical rigidity is also seen across all three standoff distances, where the secondary reflected shocks are of higher magnitude when compared to experimental recordings. The 700mm standoff present the closest agreement between experimental and numerical results, deduced to be a result of free-water shock propagation and is not influenced by any near-field variability or interface issues. Due to the difficulty in prescribing exactly where the end of the positive phase is, 0.4ms after the shock arrival has been deemed appropriate as cutoff point for all traces for comparative assessments. The secondary pulses are not considered for further analysis; however, it is noted that the difference in predicted arrival time evident at 400mm stand-off was also evident at 700mm. If this secondary pulse were important for operational reasons, then further consideration would be merited, however for our purposes only the larger energy and magnitude primary pressure shock pulse is further analysed.

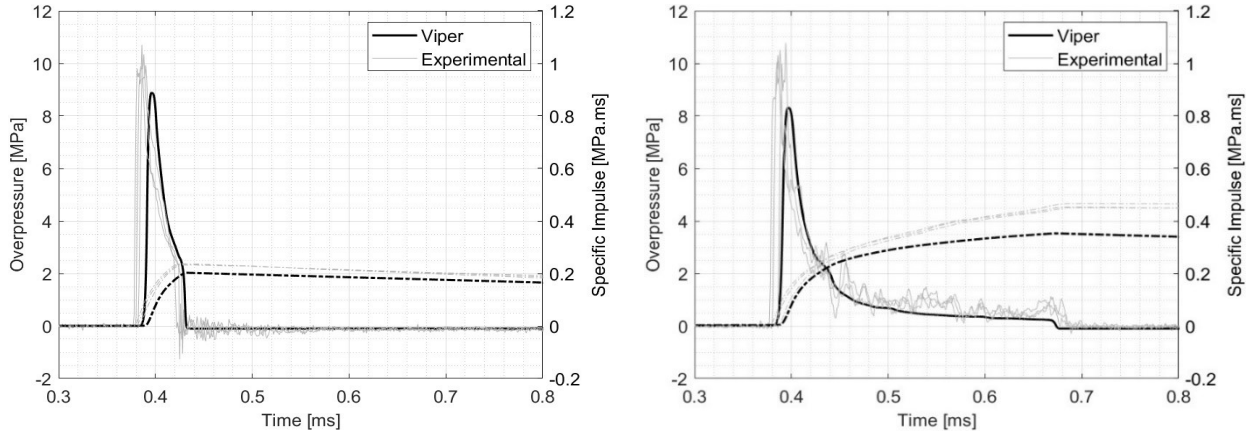

Figure 4. Pressure-time and specific impulse time history profiles for 5g PE10 spherical charge detonated centrally of the UoS UNDEX tank filled with 1m of water and sand-bed strata. Comparisons made between gauge type recordings and Viper UNDEX simulations at a standoff of 600mm and depths 40mm (Left) and 350mm (Right).

For a depth variable assessment, the experimental trial used gauges positioned at a consistent standoff distance of 600mm (assumed to be unaffected by near-field variability), but with varying position in depth below the water surface from 40-985mm within a 1m body of water and the charge detonated central to the tank and at 500mm height (denoted by gauge layout 2 in Figure 1). Specific considerations have been made for traces closer to the water-air interface to evaluate the extent to which the numerical solver can capture cavitation phenomena, where the shock wave interacts with the water-air interface and due to water being unable to retain considerable tensile loads, a drop off in pressure is experienced.

Figures 5a-c represent direct comparisons between resulting positive phase blast parameters from both analysed experimental and numerical data sets. The three parameters investigated are arrival time of the initial shock wave, the peak overpressure and the subsequent specific impulse values. Figure 5 indicates that the velocity at which the shock wave travels within the water medium is capture remarkably well, with a near-perfect 1:1 relationship between experimental and numerical values. For overpressure and impulse values there is considerably more divergence. This is due to cell size within the numerical simulation which can round off peak overpressures, as seen in both Figures 5a and 5b. Within each figure, gauge positioning has been discretised into coloured markers which represent different physical shock behaviour within the positive phase each will be discussed independently. Each test scenario is now analysed in more detail to understand why the predictions diverge from the experiments. It is important to note that experimental data has not been filtered and has been batch processed, therefore the consistency could be further improved with more rigorous curve fitting techniques which has been validated in air shock characterisation [11].

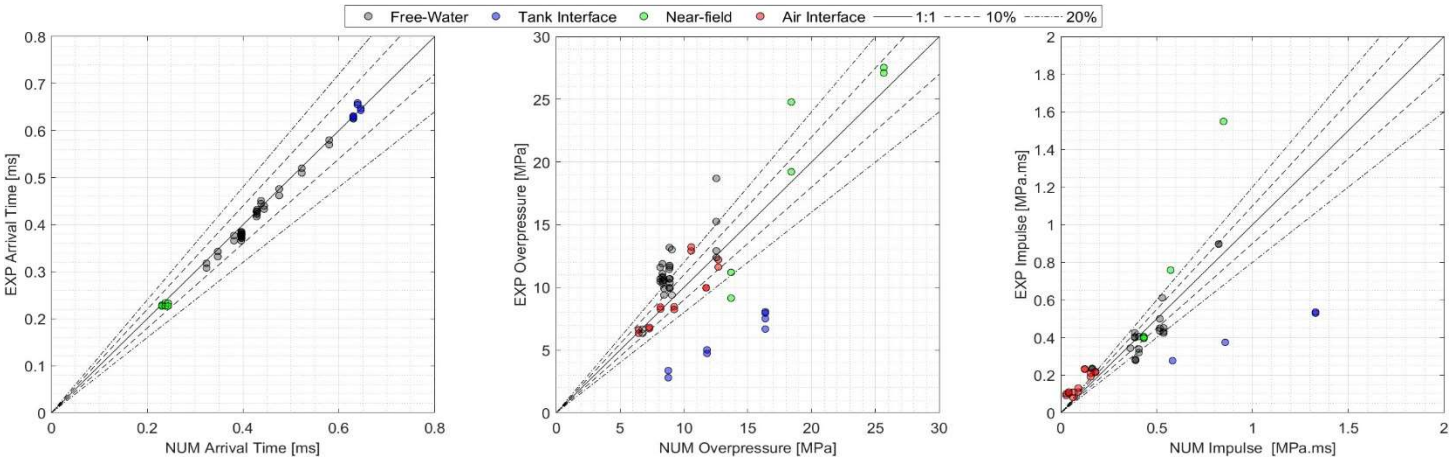

Figure 5. Experimental data against numerical output for a) Arrival time, b) peak overpressure and c) maximum specific impulse recorded consistently at 0.4ms after the shock arrival.

First the simplest of cases, namely free water (black markers) whereby no interaction with any interface is experienced within the positive phase is considered. The gauge locations within the simulations that were remote from any interface boundary captured the form of the shock wave with reasonable levels of accuracy.

Secondly, for gauges at the water-air interface, a similar comparison between numerical and experimental is recorded which validates the solvers' ability to capture cavitation behaviour as seen in Figure 5a.

Next, towards the tank-water interfaces the assumption of rigid reflection from the side wall of the tank lead to a significant pressure wave traveling inwards towards the centre which was not evident in the experimental traces. The experimental detonations would, in reality, exhibit significant energy dissipation due to tank-water interaction.

Finally, gauges with close proximity to the detonation point exhibited much higher experimental impulses than those was predicted numerically. This was attributed to the physical recording limitation of the gauge itself. Due to the spherical nature of the expanding shock front interacting with a long thin rod-like PCB gauge, the shock loading is progressive as each part of the shock arrives as the gauge face. The green markers within 0.4m of the detonation centre at which point the shock which interacts with the centre of the gauge

begins to unload before the same shock arrives at the two ends of the gauge. This means that an artificially higher loading, and higher impulse, would be induced for gauges at this distance and closer. The green marker which shows agreement between experimental and numerical results when using the Neptune gauge at 0.4m, a much smaller point source-like probe which compares more closely to that of a numerical gauge point.

Conclusion

This paper offers experimental validation to the new numerical underwater explosion prediction tool developed by Viper::Blast. Comparisons have been made to well controlled small scale underwater explosive experiments conducted at the University of Sheffield and reported in detail within [6]. With all the experimental-to-numerical limitations identified, it is possible to say, for regions of measurement which theoretically should agree with one another, there is a maximum +/- 20% spread for pressure and impulse recordings and less than +/-5% for arrival time of the incident shock wave. This provides significant developments in the ability to predict loading conditions within underwater environments as a result of explosive loading with a much less computational expensive methodology than traditional used.

References

1. A. Chester et al (2024), **A comparison of far-field explosive loads by a selection of current and emerging blast software**. *International Journal of Protective Structures. 2024;0(0).*
2. A. A. Dennis and S. E. Rigby (2024). **The Direction-encoded Neural Network**: **A machine learning approach to rapidly predict blast loading in obstructed environments**. *International Journal of Protective Structures. 2024;15(3):455-483*
3. P. R. Nowak et al (2023). **Experimental verification of different analytical approaches for estimating underwater explosives**, *International Journal of Protective Structures 2023 14:4, 571-583*
4. P. R. Nowak, et al. (2023), **Small-scale underwater explosion in shallow-water tank,** *Ocean Engineering,* Volume 288, Part 1,2023,115894,
5. R.H. Cole (1948). **Underwater Explosions**. Princeton University Press, Princeton.
6. D. G. Farrimond et al. (2024**), Characterisation of Underwater Shock Parameters in Shallow and Open Water Conditions**, *ISIEMS19, Bonn, Germany, 2024*
7. D. G. Farrimond et al (2024). **Far-field positive phase blast parameter characterisation of RDX and PETN based explosives**. *International Journal of Protective Structures*;15(1):141-165.
8. A. B. Wardlaw Jr and J. A. Luton (2000), **Fluid-Structure Interaction Mechanisms for Close-In Explosions,** Shock and Vibration 7, 265–275
9. A.L Brundage, **Implementation of Tillotson Equation of state for hypervelocity Impact of Metals, Geologic Materials, and Liquids**, Procedia Engineering Vol 58, Page 2013, Pages 461-470
10. A. Kapahi et al. (2015), **A multi-material flow solver for high speed compressible flows** *Computers & Fluids*, 115, 25–45
11. D. G. Farrimond et al. (2022) **Time of arrival as a diagnostic for far-field high explosive blast waves.** I*nternational Journal of Protective Structures*. 2022;13(2):379-402.